EFFECT OF CRACK CURVING ON STRESS INTENSITY FACTOR/ENERGY RELEASE RATE IN THREE-POINT BEND SPECIMENS

B.L. Karihaloo*

The influence of crack curving/kinking on the stress intensity factor and energy release rate at the tip of a notch in three-point bending is studied. Expressions for these fracture parameters are developed on the basis of the true state of stress ahead of the notch tip. The notch front which may kink/curve under the influence of the shear stress component is assumed to propagate along the direction of vanishing minor stress intensity factor. It is shown that the resulting expressions for the stress intensity factor and energy release rate are similar to ASTM formulae. However the fracture toughness predicted by these expressions is consistently higher than that computed from the ASTM formulae.

INTRODUCTION

The formulae for the determination of fracture toughness from three-point bend specimens proposed by Brown and Srawley (1), Srawley and Gross (2), and Srawley (3) and adopted by ASTM imply that the state of stress immediately ahead of the pre-crack front is one of pure tension, so that the crack front will not deviate from its initial (straight) path. Any small deviation from the straight path is unlikely to make a substantial difference to the resulting fracture toughness and may therefore be ignored. There are many instances, however, where the deviation may not be insignificant. This is likely to be so not only in the case of hetrogeneous materials such as concrete, reinforced ceramics (see, e.g. Nallathambi et al (4), (5)) but also in homogeneous materials because of a complex state of stress immediately ahead of the pre-crack front.

The true stress state at the tip of a pre-crack in a three-point bend specimen consists of not only a tensile stress normal to the crack faces but also of a significant (tensile) stress in the

* School of Civil and Mining Engineering, Sydney University, N.S.W. 2006, Australia.

plane of the crack and of a shear stress. In fact elastic finite element calculations show that the in-plane normal and shear stresses can be comparable in magnitude with the normal stress. It is now generally accepted (see, e.g. Karihaloo et al (6), Cotterell and Rice (7), Karihaloo et al (8), Hayashi and Nemat-Nasser (9), and Karihaloo (10) that the in-plane normal stress component controls the stability of the crack growth (a tensile in-plane stress enhances this growth, whereas a compressive in-plane stress retards it), whilst the shear stress component forces the crack front to deviate from its straight path, producing a kinked/curved crack front.

It seems appropriate therefore to modify the ASTM formulae for three-point bend specimens by making an allowance for the true stress state ahead of the pre-crack front. This has been achieved in the present work. Similar modification may be possible for compact-tension specimens, but this is not pursued here.

The modification has been accomplished by calculating the stress intensity factor and energy release rate not at the tip of the straight crack itself but at the tip of an infinitesimally small kink that is likely to form at the crack front in presence of the complex state of stress. The kink is assumed to form in the direction along which the minor stress intensity factor vanishes. This criterion is, of course, almost equivalent to the maximum energy release rate criterion (6, 9). The resulting compliance functions are shown to depend explicitly on both the notch/depth and the span/depth ratios. The compliance functions proposed here, however, retain the simplicity of the functions in the original ASTM formulae.

STRESS INTENSITY FACTOR AND ENERGY RELEASE RATE

In order to calculate the stress intensity factors and the energy release rate at the tip of a crack, it is argued that the true state of stress ahead of it must be considered and an allowance must be made for the possible formation of a kink. Let k_1 and k_2 denote the stress intensity factors at the tip of an existing plane crack and let G denote the energy release rate. Furthermore, let k_i^* (i=1,2) and G^* denote the corresponding non-dimensional fracture parameters, such that

$$k_i^* = k_i/(\sigma_o\sqrt{a}), \qquad G^* = G/(\sigma_o^2\, a/E), \tag{1}$$

where $\sigma_o = 6M/(bd^2)$ is the nominal flexural stress in an unnotched three-point bend specimen and a is the initial notch depth. Here, $M = PL/4$ is the maximum bending moment due to the mid-span load P, and b, d and L are, respectively, the width, depth and span of the beam. Then taking into account σ_{xx} and σ_{xy} besides σ_{yy} and allowing for the possible deviation of the existing crack front from its

plane, it may be shown (7-11) that the non-dimensional stress intensity factors and energy release rate at the tip of an incipient, infinitesimally small kink are given by

$$K_I^* = K_{11}\, k_1^* + K_{12}\, k_2^*, \tag{2}$$

$$K_{II}^* = K_{21}\, k_1^* + K_{22}\, k_2^*, \tag{3}$$

$$G^* = G_{11}\, k_1^{*2} + G_{12}\, k_1^*\, k_2^* + G_{22}\, k_2^{*2}. \tag{4}$$

The coefficients $K_{\alpha\beta}$ and $G_{\alpha\beta}$ ($\alpha,\beta = 1,2$) depend on the in-plane stress and the kink angle θ (9). The above expressions are strictly speaking applicable to semi-infinite bodies and are therefore only a reasonable approximation to the finite beam specimens under consideration.

The expressions (2) - (4) relate the stress intensity factors K_I^*, K_{II}^* and the energy release rate G^* at the tip of the incipient kink to the stress intensity factors k_1^* and k_2^* at the tip of the pre-existing notch. For small values of the kink angle θ it is possible to express $K_{\alpha\beta}$ and $G_{\alpha\beta}$ explicitly in terms of the kink angle and the in-plane normal stress σ_{xx} (9, 10). It has also been shown (9) that Irwin's formula relating G^* to K_I^* and K_{II}^* through $G^* = K_I^{*2} + K_{II}^{*2}$ is strictly true for all values of the kink angle θ, provided that the stress intensity factors in the formula are taken to be those at the tip of an infinitesimally small kink; the formula clearly applies after kinking has taken place.

It now generally accepted (see e.g. (6-10), and Bilby and Cardew (11), Kalthoff (12), and Lo (13)) that the kink is likely to form in the direction along which the minor stress intensity factor vanishes. This criterion is usually referred to as the criterion of local symmetry ($K_{II}^* \simeq 0$). It is known (6, 9) to be almost equivalent to the maximum energy release rate criterion according to which the crack front kinks/curves in the direction along which $\partial G^*/\partial\theta = 0$. It is also likely that both these criteria are, in turn, equivalent to the maximum stress criterion (6) and to the minimum strain energy density criterion (7). However, this aspect of the problem needs further consideration which will not be attempted here.

From the computational point of view the criterion of local symmetry is the more useful in that it is easy to determine the kink angle. It is worth pointing out that the relationship between K_I^* and G^* is not the simple quadratic one assumed in the ASTM formulation

$$K_I/(\sigma_o\sqrt{a}) = Y(\alpha;\beta), \qquad G = K_I^2/E, \tag{5}$$

where the compliance function $Y(\alpha;\beta)$ depends linearly on $\beta = L/d$ but is a polynomial in $\alpha = a/d$ (3) (for $\beta = 4 \pm 0.01$)

$$Y(\alpha;\beta) = [1.99-\alpha(1-\alpha)(2.15-3.93\alpha+2.7\alpha^2)]/[(1+2\alpha)(1-\alpha)^{\frac{3}{2}}] \qquad (6)$$

FINITE ELEMENT IMPLEMENTATION

A plane stress finite element program using eight-noded isoparametric elements (see, e.g. Owen and Hinton (14), Barsoum (15), Mazumdar and Murthy (16)) was used to analyse the three-point notched beam specimen. A study of mesh sizes was undertaken in order to arrive at an optimum mesh (Fig. 1). The depth of the beam was assumed to be constant (100 mm) and the span was varied to achieve the desired L/d ratio. Likewise, the boundary conditions along the line of symmetry (x-axis) were varied to achieve the desired a/d ratio. In all, the span/depth ratio was varied between 2 and 10, and the notch/depth ratio was varied between 0.1 and 0.7. The midspan load was chosen to be equal to 10 N so that results could be easily factored for other load values. The mesh gradation from fine near the notch tip to coarse near the supports was achieved by using a 'master-slave' technique, such that the size of the element near the notch tip was always equal to 1.00 x 1.25 mm (Fig. 1).

Details of the iterative procedure for calculating the stress intensity factor K_I^* (expression 2) and the energy release rate G^* (expression 4) at the tip of an incipient kink (which forms along $K_{II}^* \simeq 0$) will be found in Nallathambi and Karihaloo (17).

It is customary in a finite element calculation of stress intensity factors to vary r/a for a given geometry in order to extrapolate to $r/a \to 0$. This requires a lot of computational effort. In the procedure outlined above, an alternative scaling technique proposed by Kisu et al (18) was used elminating the need for varying r/a. According to this technique the stress intensity factor for a beam of given geometry is obtained by scaling with respect to a standard geometry as follows. First, it is noted that the near field stress σ_{yy} at (r,θ) may be expressed in terms of the nominal flexural stress σ_o, whereupon

$$\sigma_{yy}\sqrt{(k_1^* \surd a/(2\pi r))} = \sigma_o \qquad (7)$$

It follows from expression (7) that the ratio on the left hand side is a constant for all a/d and L/d, provided σ_o is the same for all geometries. Now a standard three-point bend problem (for which k_1^* is exactly known) is solved by the finite element programme and r chosen in such a way that the resulting k_1^* is equal to the known exact value. Then for any other geometry with the same b, d, L and σ_o but with a different notch depth a the stress intensity factor k_1^* is obtained by equating the left hand

side of equation (7) to that of the standard problem, distinguished by subscript 's', whereupon

$$k_1^* = k_{1s}^* \frac{\sigma_{yy}}{(\sigma_{yy})_s} \sqrt{\frac{r}{r_s}\frac{a_s}{a}} . \qquad (8)$$

This scaling procedure is not limited to three-point bend problems. In fact, the accuracy of the procedure was tested on a centre-cracked tension (CCT) specimen for which exact results are available in the paper by Isida (19). The standard problem was the one with a/d = 0.5. The accuracy of the present procedure may be judged from Figure 2 which compares the computed k_1^* for bend specimens with that given by ASTM formula (1).

IMPROVED COMPLIANCE FUNCTIONS

The computer algorithm and scaling procedure outlined above were used on three-point bend specimens with varying L/d (between 2 and 10) and a/d (between 0.1 and 0.7). The standard problem had L/d = 4 and a/d = 0.5 (2). A regression analysis was performed on the stress intensity factors K_I^* (note that $K_{II}^* \simeq 0$) and energy release rates G^* so computed, giving (error < 1%)

$$K_I^* = \bar{K}_I/(\sigma_o \sqrt{a}) = Y_1(\alpha)\, Y_2(\alpha,\beta), \qquad (9)$$

$$G^* = \bar{G}/(\sigma_o^2 a/E) = Z_1(\alpha)\, Z_2(\alpha,\beta), \qquad (10)$$

where α = a/d, β = L/d, and an overbar has been used to distinguish $\bar{K}_I$ and $\bar{G}$ from the corresponding ASTM parameters K_I and G (expression 5).

The various compliance functions appearing in (9) and (10) are defined as follows:

$$Y_1(\alpha) = A_0 + A_1\alpha + A_2\alpha^2 + A_3\alpha^3 + A_4\alpha^4, \qquad (11)$$

$$Z_1(\alpha) = C_0 + C_1\alpha + C_2\alpha^2 + C_3\alpha^3 + C_4\alpha^4, \qquad (12)$$

$$Y_2(\alpha,\beta) = B_0 + B_1\beta + B_2\beta^2 + B_3\beta^3 + B_4\alpha\beta + B_5\alpha\beta^2, \qquad (13)$$

$$Z_2(\alpha,\beta) = D_0 + D_1\beta + D_2\beta^2 + D_3\beta^3 + D_4\alpha\beta + D_5\alpha\beta^2. \qquad (14)$$

The regression coefficients A_i, C_i (i=0, 1, ..., 4) and B_j, D_j (j=0, 1, ..., 5) are listed in Table 1.

TABLE 1 - Regression Coefficients A_i, C_i, B_j, D_j (i=0, ..., 4) (j = 0, ..., 5) in Compliance Functions.

i/j	A_i	C_i	B_j	D_j
0	3.6460	1.5640	0.4607	1.9560
1	-6.7890	-8.3200	0.0484	0.3982
2	39.2400	52.9500	-0.0063	-0.0553
3	-76.8200	-124.9000	0.0003	0.0027
4	74.3300	122.9000	-0.0059	0.0202
5	-	-	0.0003	-0.0055

It is interesting to note that the form of compliance function $Y_1(\alpha)$ appearing in (9) is identical to that of $Y(\alpha;\beta)$ appearing in the ASTM formula (Reference (1)) and is very similar to the modified $Y(\alpha;\beta)$ (expression (6)) proposed by Srawley (3); the coefficients are naturally different in each case. It should however be pointed out that whereas the dependence of K_I^* on L/d is explicitly indicated here by the compliance function $Y_2(\alpha,\beta)$, the ASTM formulae (1-3) predict a linear dependence on L/d. It is clear from the present analysis that this dependence is non-linear, especially for small values of L/d.

Figure 3 compares the product of compliance functions $Y_1(\alpha)\ Y_2(\alpha,\beta)$ proposed in the present work with the function $Y(\alpha;\beta)$ in the ASTM formula (1). It is clear that $\bar{K}_I$ (and $\bar{G}$) which is based on the true stress state ahead of an existing notch in a three-point bend specimen is consistently larger than the corresponding K_I (and G) given by the ASTM formulae. The formulae proposed in this work should give a better estimate of $\bar{K}_I$ and $\bar{G}$, especially for hetrogeneous materials.

REFERENCES

(1) Brown, W.F. and Srawley, J.E., "Crack Toughness of High Strength Metallic Materials", ASTM-STP 410, 13, 1966.

(2) Srawley, J.E. and Gross, B., Engng. Fracture Mech., Vol. 4, 1972, pp.587-589.

(3) Srawley, J.E., Int. J. Fracture, Vol. 12, 1976, pp.475-476.

(4) Nallathambi, P., Karihaloo, B.L. and Heaton, B.S., Cement Concrete Res. Vol. 15, 1985, pp.117-126.

(5) Nallathambi, P., Karihaloo, B.L. and Heaton, B.S., Mag. Concrete Res. Vol. 36, 1984, pp.227-236.

(6) Karihaloo, B.L., Keer, L.M. and Nemat-Nasser, S., Engng. Fracture Mech., Vol. 13, 1980, pp.879-888.

(7) Cotterell, B. and Rice, J.R., Int. J. Fracture, Vol. 16, 1980, pp.155-169.

(8) Karihaloo, B.L., Keer, L.M., Nemat-Nasser, S. and Oranratnachai, A., J. Appl. Mech., Vol. 48, 1981, pp.515-519.

(9) Hayashi, K. and Nemat-Nasser, S., J. Appl. Mech., Vol. 48, 1981, pp.520-524.

(10) Karihaloo, B.L., J. Mech. Matls., Vol. 1, 1982, pp.189-201.

(11) Bilby, B.A. and Cardew, G.E., Int. J. Fracture, Vol. 11, 1975, pp. 708-712.

(12) Kalthoff, J. Proc. Third Int. Conf. on Fracture (ICF 3), Munich, Vol. X, 1973, P. 235.

(13) Lo, K.K., J. Appl. Mech., Vol. 45, 1978, pp.797-802.

(14) Owen, D.R.J. and Hinton, E., "Finite Elements in Plasticity - Theory and Practice", Pineridge Press, Swansea, U.K., 1980.

(15) Barsoum, R.S., Int. J. Num. Methods Engng, Vol. 10, 1976, pp.25-37.

(16) Mazumdar, D.P. and Murthy, P.N.,"Determination of Stress Intensity Factors Using Mixed Elements", Fracture Mech. in Engng Application. Eds. G.C. Sih and S.R. Valluri, Sijthoff & Noordhoff, The Netherlands, 1979, pp.705-714.

(17) Nallathambi, P. and Karihaloo, B.L., J. Engng. Fract. Mech. (submitted).

(18) Kisu, H., Yuuki, R. and Kitagawa, H., "Application of New Methods to the Boundary Element Method Analysis of Stress Intensity Factors. Advances in Fracture Res. Proc. ICF6, Eds. S.R. Valluri et al. Pergamon Press, Vol. 2, 1984, pp.927-936.

(19) Isida, M., Int. J. Fracture Mech., Vol. 7, 1971, pp.301-316.

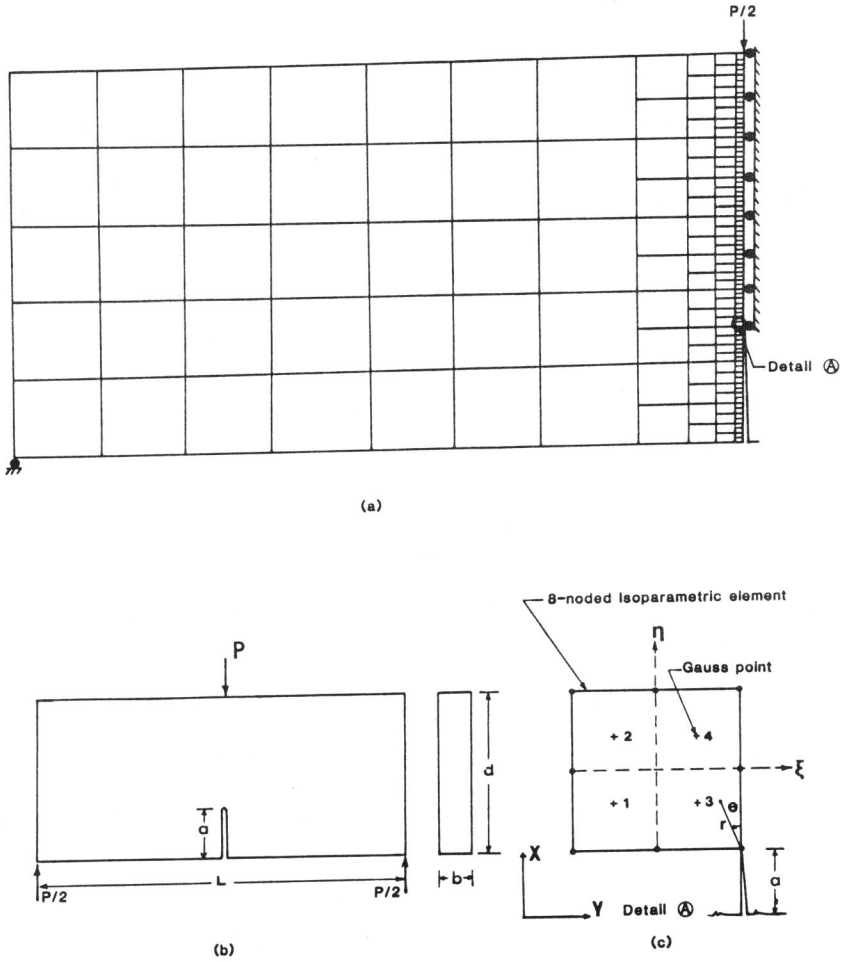

Figure 1 Finite element mesh distribution over one half (a) of the three point bend specimen (b). Detail of the element ahead of the notch tip is shown in (c).

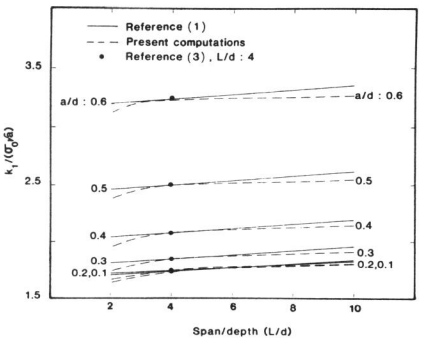

Figure 2 Comparison of normalised stress intensity factor in pure tension field calculated by the present finite element program with the ASTM formula.

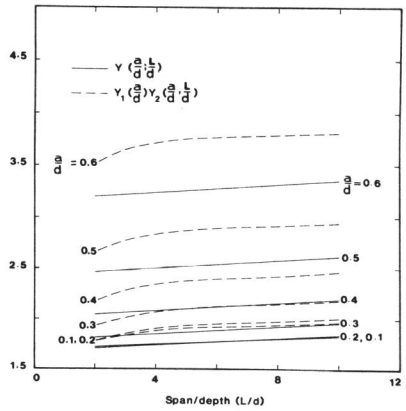

Figure 3 Comparison of compliance function for stress intensity factor K_I proposed in the present work with the compliance function for K_I.